

DNA Methylation Associated with Repeat-Induced Point Mutation in *Neurospora crassa*

MICHAEL J. SINGER,[†] BEN A. MARCOTTE, AND ERIC U. SELKER*

Institute of Molecular Biology, University of Oregon, Eugene, Oregon 97403

Received 9 June 1995/Returned for modification 17 July 1995/Accepted 20 July 1995

Repeat-induced point mutation (RIP) is a process that efficiently detects DNA duplications prior to meiosis in *Neurospora crassa* and peppers them with G:C to A:T mutations. Cytosine methylation is typically associated with sequences affected by RIP, and methylated cytosines are not limited to CpG dinucleotides. We generated and characterized a collection of methylated and unmethylated *am*^{RIP} alleles to investigate the connection(s) between DNA methylation and mutations by RIP. Alleles of *am* harboring 84 to 158 mutations in the 2.6-kb region that was duplicated were heavily methylated and triggered de novo methylation when reintroduced into vegetative *N. crassa* cells. Alleles containing 45 and 56 mutations were methylated in the strains originally isolated but did not become methylated when reintroduced into vegetative cells. This provides the first evidence for de novo methylation in the sexual cycle and for a maintenance methylation system in *Neurospora* cells. No methylation was detected in *am* alleles containing 8 and 21 mutations. All mutations in the eight primary alleles studied were either G to A or C to T, with respect to the coding strand of the *am* gene, suggesting that RIP results in only one type of mutation. We consider possibilities for how DNA methylation is triggered by some sequences altered by RIP.

Certain cytosines in the DNA of many animals, plants, and fungi are methylated. The importance of DNA methylation in mice is highlighted by the finding that it is essential for embryogenesis (24). Many clues to the function(s) of methylation are emerging. DNA methylation has been implicated in X-chromosome inactivation (49), genomic imprinting (4, 38), and other processes. Methylation of promoter sequences typically correlates with gene inactivity (1); however, it is unclear to what extent methylation is used by eukaryotic organisms to regulate transcription.

Despite progress made in understanding functions of DNA methylation, little is known about the control of methylation in eukaryotes. In mammals, DNA methylation patterns are reorganized during gametogenesis and embryogenesis (28), but the patterns are relatively stable after differentiation of tissues. 5-Methylcytosine (m⁵C) is predominantly located within CpG dinucleotides in animals (50). Riggs (36) and Holliday and Pugh (20) proposed that a “maintenance methylase” propagates methylation patterns by acting on hemimethylated 5'-CpG-3'/GpC dinucleotides in newly replicated DNA. Aspects of this model have been supported, but non-CpG methylation (54, 60) and methylation heterogeneity evidenced by partially methylated sites (56, 63) challenge the model (39). How methylation patterns are first established also remains largely a mystery, although results of recent studies in mammals suggest that binding of the transcription factor Sp1 can keep regions unmethylated (5, 25).

The fungus *Neurospora crassa* provides an excellent system to study DNA methylation. Most of the genome appears devoid of methylation; however, several densely methylated endogenous sequences have been described, including the ζ - η

and ψ 63 regions and the tandemly organized genes coding for rRNA (rDNA) (14, 32, 37, 47). The ζ - η (17) and ψ 63 regions (25b) and most or all other methylated sequences in *N. crassa* (39a) appear to be relics of repeat-induced point mutation (RIP). RIP is a premeiotic process that detects sequence duplications and then makes numerous G:C to A:T mutations in both duplicated sequences (7, 40, 41). Methylation is typically, but not invariably, associated with products of RIP (41, 44).

DNA methylation in *N. crassa* has several interesting features. First, m⁵C is neither limited to CpG dinucleotides (47) nor preferentially located in any particular oligonucleotide sequence (43). Second, the methylation pattern in methylated sequences is highly heterogeneous in clonal cultures (47). Third, at least some methylated chromosomal regions contain portable signals for de novo methylation (e.g., ζ - η , ψ 63, and an allele of *flank* that arose by RIP in the laboratory), as demonstrated by DNA-mediated transformation experiments (8, 26, 41). De novo methylation occurred after these products of RIP had been cloned, amplified in *Escherichia coli* (thereby stripping them of methylation), and then reintroduced into vegetative *N. crassa* cells. These observations suggested that *N. crassa* has an active de novo methylation system in vegetative cells and possibly no maintenance methylase.

To investigate how point mutations cause methylation, we induced RIP in the NADP-specific glutamate dehydrogenase (*am*) gene and characterized methylated and unmethylated *am* alleles at the DNA sequence level. We reasoned that this collection of *am* alleles would illustrate what distinguishes methylated from unmethylated DNA in the *Neurospora* genome, thereby providing insight into how methylation is controlled. The *am* gene was chosen because it is well characterized and because a method for targeted gene replacement at *am* had been developed (26). We also asked whether the methylation detected in the new *am* alleles reflected creation of signals for de novo methylation or action of a maintenance methylation mechanism. Evidence of both was obtained.

* Corresponding author. Mailing address: Institute of Molecular Biology, University of Oregon, Eugene, OR 97403. Phone: (503) 346-5193. Fax: (503) 346-5011. Electronic mail address: selker@oregon.uoregon.edu.

[†] Present address: Department of Molecular Biotechnology, University of Washington, Seattle, WA 98195.

MATERIALS AND METHODS

Strains, culturing of *N. crassa*, DNA isolation, and Southern hybridization.

Transformant T-510-5.6 (44), a strain containing an ectopic copy of *am*, was crossed with strains containing a copy of *am* at the native location (N150 or J857) to produce strains (N250, N276, and N277) with two functional copies of *am* (see Table 1). T-510-5.6 was crossed to tester strains, and the ectopic copy of *am* showed $\approx 1.2\%$ linkage to *pan-2* and $\approx 10\%$ linkage to *ylo-1* (on linkage group VI; data not shown). The *am* allele in N617 (*am*^{RIP8}) was referred to as *am*^{RIP-SM} elsewhere (43).

N. crassa was cultured by standard methods (9). Procedures for DNA isolation and Southern hybridization were described previously (14). For the 5-azacytidine (5AC) experiments, liquid media containing 2% sucrose, 1 \times Vogel's salts, the appropriate amino acid supplements, inositol, and 24 μ M 5AC were inoculated with a loop of conidia and incubated at 25°C for 40 h with shaking at 250 rpm.

Plasmids for targeted transformation. The 5.2-kb *Pst*I-*Hind*III fragment of pJR3, including the *am* gene, was inserted into a modified pTZ18U vector (with the *Bam*HI and *Eco*RI sites destroyed by filling in) to create pMS2. Fragments of approximately 2.7 kb from *am*^{RIP3}, *am*^{RIP4}, *am*^{RIP5}, *am*^{RIP7}, and *am*^{RIP8} alleles were amplified by PCR and cleaved with *Bam*HI. The 2.6-kb *Bam*HI fragments of these mutant alleles were then substituted for the same fragment in pMS2 to create pMS8, pMS10, pMS12, pMS13, and pBM7, respectively. Targeted transformation was performed as described previously (26).

PCR and sequencing. Alleles of *am* occupying the native site were amplified with primers outside the duplicated region (nucleotides 62 to 2624). PCR products were sequenced directly, as described elsewhere (43), except that PCR products of *am*^{RIP1} were sequenced at Oregon State University Central Facilities by using the dye incorporation method and an ABI automated sequencer. The following oligonucleotides were used for PCR and sequencing (*am* sequence coordinates in parentheses): GTCCAGGCGTTCCCATGTTC (-79 to -60), GATCCGATGTCACGGACAAG (2 to 21), CGAGAYAAGAYAGACGGA AT (93 to 74), GAAAGCTGTGCCCTCTCTGG (213 to 232), GCCTGCTC GAATCGGGCTC (376 to 357), GCGTGCATTTCAGTTCCGTG (536 to 555), GGTTGACCTGGACGTTGCGC (594 to 575), TCCGTCAACCTTTC CATTCT (660 to 679), GCGCTTTCATGGCCGAGCTT (866 to 885), GTTA CCGTCTTGTTTACTAC (1058 to 1077), GGGCAACGCGCTTGCCAGCG (1135 to 1116), CTGGAAGCTGTAAGGGACT (1320 to 1301), TTCGTGCTG CTGAGGGTTC (1459 to 1478), TTGAGAACAACCGCAAGGAG (1511 to 1530), TTGCGGTTGTTCTCAAAGAC (1526 to 1507), GACTCAGGCT GAGGTTGACG (1635 to 1654), GGAAGCTCGCCCTCAGCAGC (1742 to 1723), AATGGTGTGATTTACCGTT (1830 to 1849), TTTAATRAGAATR GAAA (1848 to 1864), AACTCCGGCCCGTGATTTTC (1923 to 1904), ACA TTTATTGACGTCCAATT (2160 to 2141), GTTRGTACCCGAGCTTTRG (2271 to 2290), CATGATCAGGTGTTGTCTGC (2359 to 2340), TCGTTRGY ATRACTCGAGAT (2553 to 2572), AGAGAGCATCGTCTCAAAGC (2669 to 2650).

Computerized sequence analyses. Window analyses and other standard analyses were performed with the University of Wisconsin Genetics Computer Group Software Package. The sequences of 97 nonribosomal *N. crassa* genes, totaling 210 kb, were used as controls. Their GenBank names are as follows: NEU16DNA, NEUACU5, NEUACU8, NEUALIA, NEUAL3, NEUALCA, NEUAM, NEUAMG, NEUAMM, NEUAMTR, NEUATPASE, NEUATPC, NEUATPPM, NEUATPPRO, NEUCAM, NEUCON13, NEUC11, NEUCOMPI, NEUCON10A, NEUCON8, NEUCOX4, NEUCOX5, NEUCOX6, NEUCPC, NEUCRPIG, NEUCRP2, NEUCRP3, NEUCYCGEN, NEUCY CLO, NEUCYT21, NEUCYT1R, NEUCYTCG, NEUCYTCR, NEUGR G1G, NEUH341, NEUH342, NEUHIS3, NEUHSP30, NEULCC, NEULCA, NEULCCB, NEULEURS, NEULEURSC, NEULEURSD, NEUMET, NEU METC, NEUMETCA, NEUMOM72, NEUMPPX, NEUMTA1A, NEUMUT, NEUNADGDH, NEUNC01, NEUNDU51, NEUNDU78, NEUNHU18, NEU NIT4A, NEUNUC1, NEUNUO12, NEUNUO32, NEUNUO40, NEUNUO49, NEUNURI, NEUODC, NEUODCA, NEUPEP, NEUPHO4A, NEUPHR, NEUPORIN, NEUPSAS, NEUPYR4, NEUPYR4G, NEUQA, NEUQA1SRA, NEUQA2WT, NEUQA4, NEUQAX2, NEUQAX3, NEURAS, NEURIPB1, NEURIPB2, NEURPSSU, NEUSOD1, NEUTGFF3, NEUTGL, NEUTRP1, NEUTRP3A, NEUTUBB, NEUTYRA, NEUTYRB, NEUTYRSM, NEU UBI3, NEUUBQ, NEUCYCR, NEUVMA1A, NEUVMA2A, and NEUXXX.

The Gentben program, which was kindly provided by John Anderson (Purdue University), was used to calculate DNA bending from nucleotide sequence (see reference 58). The algorithm for calculating bending uses parameters of the wedge model for bent DNA (57). The ENDS ratio, defined as the ratio of contour length of a nucleotide segment along the axis to the shortest distance between ends of the segment, is the measure of curvature. ENDS ratios were computed at a window width of 120 nucleotides and at a window step of 10 nucleotides.

The Thermodyn program, which was kindly provided by David Kowalski (27), was used to examine helical stabilities of methylated and unmethylated *am* alleles generated in this study.

Two programs were used to search for oligonucleotide signal sequences. The Cohomology program, which was kindly provided by David Hagen (University of Oregon), was used to search for oligonucleotide sequences of specified lengths that were common to alleles *am*^{RIP5}, *am*^{RIP6}, *am*^{RIP7}, and *am*^{RIP8}. The program

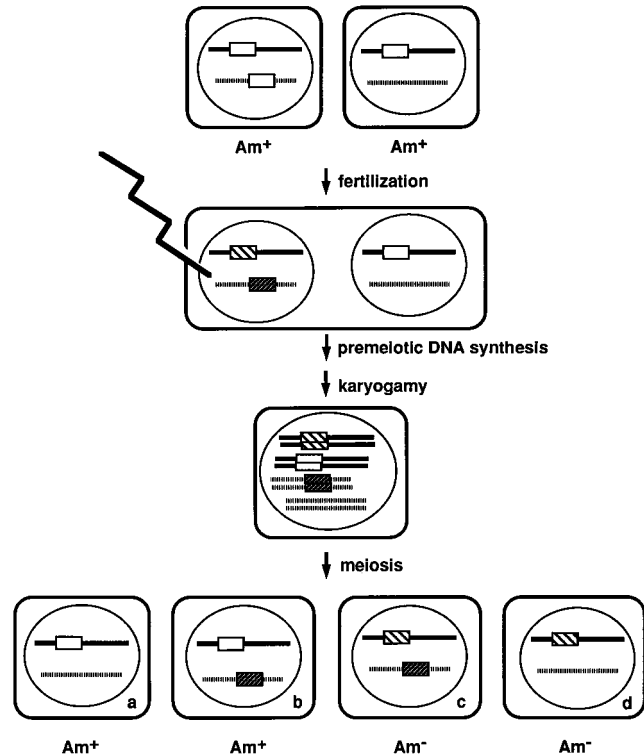


FIG. 1. Diagram of RIP in the *Neurospora am* gene. Two haploid strains of opposite mating types are illustrated, one containing an unlinked 2.6-kb duplication including the *Neurospora am* gene (open boxes). For clarity, only two chromosomes are shown. The native allele of *am* is on chromosome V (solid line), and the ectopic copy is on chromosome VI (dashed line [48a]). The lightning bolt indicates the time that RIP occurs, and the filled boxes indicate new alleles of *am* created by RIP. The four possible combinations of chromosomes in progeny are represented in the panels labeled a to d, and the expected phenotypes are indicated below them.

discarded all sequences that were found in any of wild-type *am*, *am*^{RIP1}, *am*^{RIP2}, *am*^{RIP3}, or *am*^{RIP4}. The reverse searches were also performed. We searched for 5- to 20-bp sequences, allowing zero to six mismatches. Candidate sequences were then sought in published *Neurospora* gene sequences known to be methylated or unmethylated. "Signal" (25a) operates similarly; however, a maximum of two mismatches was allowed, and the sequences of several other methylated and unmethylated *Neurospora* genes were included in the searches (ζ - η and ψ 63 were included in the methylated group, and *acu8*, *cpc-1*, *cys-3*, *mt a-1*, *mtr*, θ , *tub-2*, and the *qa* gene cluster were included in the unmethylated group).

Nucleotide sequence accession numbers. The data base accession numbers assigned by GenBank to *am*^{RIP1} through *am*^{RIP8} are, respectively, U32099 through U32106.

RESULTS

Isolation and characterization of *Am*⁻ strains. To generate a collection of *am* alleles resulting from RIP, we crossed an *am*⁺ nonduplication strain with strains containing, in addition to the native *am* gene, an ectopic functional copy of the *am* gene introduced by transformation (44) (Fig. 1). Two classes of *Am*⁻ progeny were expected, i.e., one class with two defective copies of *am* and the other class with a defective allele of *am* at the native site only. We screened progeny for the *Am*⁻ phenotype and assayed the mutant strains for methylation at *am* by Southern hybridization, using the isoschizomers *Mbo*I and *Sau*3AI. Both enzymes cut unmethylated GATC sites, but only *Mbo*I can cut when a cytosine in the site is methylated (29). *Mbo*I digests were also used to determine *am* copy number and to provide a first indication of mutations by RIP. The *am* gene is contained within a 2.6-kb *Bam*HI fragment that is

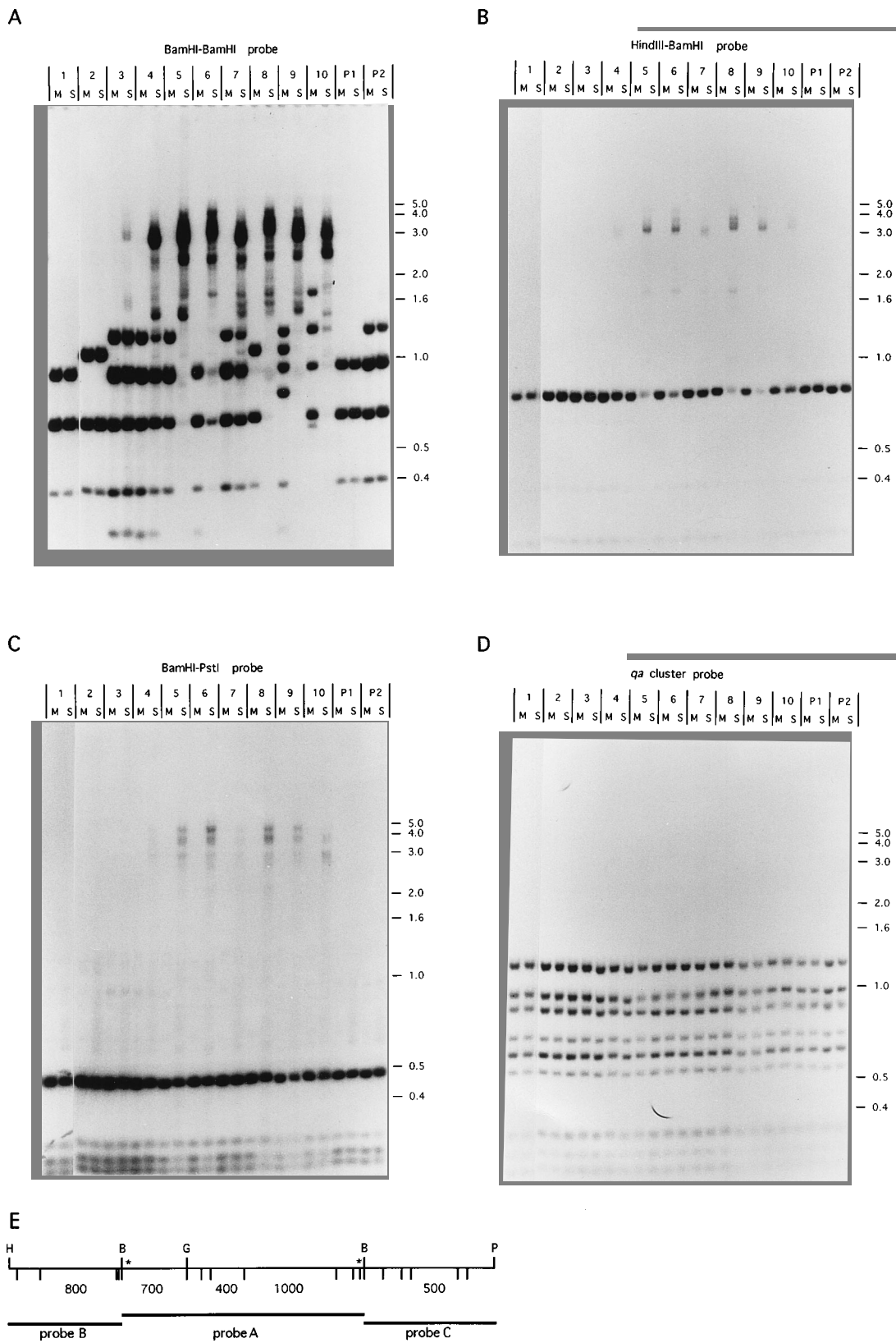


FIG. 2. Extensive DNA methylation in *am^{RIP}* alleles. (A to D) Southern hybridizations. Genomic DNA samples of strains N664 (*am^{RIP1}* [lanes 1]), N665 (*am^{RIP2}* [lanes 2]), N666 (*am^{RIP3}* [lanes 3]), N669 (*am^{RIP4}* [lanes 4]), N672 (*am^{RIP5}* [lanes 5]), N675 (*am^{RIP6}* [lanes 6]), N676 (*am^{RIP7}* [lanes 7]), N617 (*am^{RIP8}* [lanes 8]), N679 (*am^{RIP9}* [lanes 9]), N680 (*am^{RIP10}* [lanes 10]), N150 (P1), and N276 (P2) were digested with *Mbo*I (M) or *Sau*3A1 (S), processed for Southern hybridization, and probed with radiolabeled fragments from the 2.6-kb *Bam*HI fragment including the entire *am* coding region (A), the 1.2-kb *Hind*III-*Bam*HI fragment from the *am* upstream region (B), the 1.4-kb *Bam*HI-*Pst*I fragment from the downstream region of *am* (C), and the 7-kb *Pst*I fragment from the quinic acid (*qa*) gene cluster (D). The positions of molecular size standards (in kilobases) are shown. (E) Map of the wild-type *am* region showing restriction sites for *Hind*III (H), *Bam*HI (B), *Bgl*II (G), and *Pst*I (P) above the thin horizontal line. *Mbo*I-*Sau*3A1 sites with expected lengths of *Mbo*I fragments (in base pairs) corresponding to visible bands are indicated below the thin line. The thick lines depict the probes used in the indicated panels (A to C), and the asterisks indicate the boundaries of the duplication.

TABLE 1. *N. crassa* strains used^a

| Strain | Native <i>am</i> | Ectopic <i>am</i> | Other marker(s) | Derivation | Source or reference |
|--------|----------------------------|------------------------------|------------------------------------|--------------|-----------------------|
| N39 | WT | None | <i>A; fl</i> | | Laboratory collection |
| N113 | WT | None | <i>A; cot-1; inl; trp-1; ylo-1</i> | | FGSC 1987 |
| N150 | WT | None | <i>A</i> | | FGSC 2489 |
| N250 | WT | WT | <i>a; cot-1; inl; lys-1</i> | N268 × J857 | Laboratory collection |
| N261 | WT | None | <i>A; lys-1</i> | | J. Kinsey |
| N262 | WT | None | <i>a; lys-1</i> | | J. Kinsey |
| N268 | None | WT | <i>a; inl</i> | T-510 5.6 | 44 |
| N276 | WT | WT | <i>a</i> | N268 × N150 | Laboratory collection |
| N277 | WT | WT | <i>A</i> | N268 × N150 | Laboratory collection |
| N408 | WT | None | <i>A; lys-1</i> | | Laboratory collection |
| N617 | <i>am</i> ^{RIP8} | None | <i>a; lys-1</i> | N276 × N261 | 43 |
| N662 | <i>am</i> ^{RIP8} | None | <i>A; lys-1</i> | N408 + pBM7 | This study |
| N663 | <i>am</i> ^{RIP8} | None | <i>A; lys-1</i> | N408 + pBM7 | This study |
| N664 | <i>am</i> ^{RIP1} | None | <i>A; cot-1; trp-1 ylo-1</i> | N276 × N113 | This study |
| N665 | <i>am</i> ^{RIP2} | None | <i>a; inl; lys-1</i> | N250 × N39 | This study |
| N666 | <i>am</i> ^{RIP3} | <i>am</i> ^{RIPec3} | <i>a; inl; lys-1</i> | N250 × N39 | This study |
| N667 | <i>am</i> ^{RIP3} | None | <i>A; lys-1</i> | N408 + pMS8 | This study |
| N668 | <i>am</i> ^{RIP3} | None | <i>A; lys-1</i> | N408 + pMS8 | This study |
| N669 | <i>am</i> ^{RIP4} | <i>am</i> ^{RIPec4} | <i>a; lys-1</i> | N277 × N262 | This study |
| N670 | <i>am</i> ^{RIP4} | None | <i>A; lys-1</i> | N408 + pMS10 | This study |
| N671 | <i>am</i> ^{RIP4} | None | <i>A; lys-1</i> | N408 + pMS10 | This study |
| N672 | <i>am</i> ^{RIP5} | <i>am</i> ^{RIPec5} | <i>A; lys-1</i> | N277 × N262 | This study |
| N673 | <i>am</i> ^{RIP5} | None | <i>A; lys-1</i> | N408 + pMS12 | This study |
| N674 | <i>am</i> ^{RIP5} | None | <i>A; lys-1</i> | N408 + pMS12 | This study |
| N675 | <i>am</i> ^{RIP6} | None | <i>A; cot-1; inl; lys-1</i> | N250 × N39 | This study |
| N676 | <i>am</i> ^{RIP7} | <i>am</i> ^{RIPec7} | <i>A; lys-1</i> | N277 × N262 | This study |
| N677 | <i>am</i> ^{RIP7} | None | <i>A; lys-1</i> | N408 + pMS13 | This study |
| N678 | <i>am</i> ^{RIP7} | None | <i>A; lys-1</i> | N408 + pMS13 | This study |
| N679 | <i>am</i> ^{RIP9} | <i>am</i> ^{RIPec9} | <i>a; lys-1</i> | N276 × N261 | This study |
| N680 | <i>am</i> ^{RIP10} | <i>am</i> ^{RIPec10} | <i>a; lys-1</i> | N277 × N262 | This study |

^a WT, wild type; FGSC, Fungal Genetic Stock Center.

slightly longer than the duplicated region (62 bp longer upstream of *am* and 20 bp longer downstream of *am* [14a]). The wild-type *am* gene includes nine *MboI*-*Sau3AI* sites yielding three *MboI* fragments (400, 700, and 1,000 bp) that are readily detectable by Southern hybridization (Fig. 2). An additional 1.4-kb *MboI* band, which is indicative of the ectopic copy of *am*, is visible in blots of the two-copy parent and mutant strains N666, N669, N672, N676, N679, and N680 (Fig. 2; Table 1). Novel *MboI* fragments were detected in 51 of 65 *Am*⁻ strains, reflecting point mutations at *MboI*-*Sau3AI* sites (sequence data presented below). Strains N617, N665, N666, N669, N679, and N680 are examples of this class (Fig. 2).

No DNA methylation was detected at *Sau3AI* sites in *am* genes of the parent strains, in agreement with results of previous experiments (44). In contrast, of 59 *Am*⁻ progeny examined by Southern hybridization, all but four showed methylation at *am*, and the methylation was generally very heavy (all sites tested were blocked in >80% of the molecules; data not shown). We chose 10 strains that appeared to represent the full range of methylation levels for detailed analyses. Mutants N664 and N665 were chosen to represent strains with no apparent methylation. In each of these, no methylation was detected at 42 sites in the *am* region, including *Sau3AI* (Fig. 2A), *BglIII* (Fig. 3A), *MspI* (Fig. 3C), *AatII*, *AvaI*, *BamHI*, and *HpaII* sites (data not shown). Two single-copy strains (N617 and N675) and six two-copy strains (N666, N669, N672, N676, N679, and N680) were chosen to represent the methylated class (Fig. 2A). The methylation at *am* in N666 is light, as indicated by the similarity between the hybridization patterns obtained with *Sau3AI* and *MboI*. In contrast, differences between *MboI* and *Sau3AI* digestion products revealed heavy methylation in strain N617. To control for complete digestion,

all blots made in this study were stripped and reprobed with DNA from an unmethylated region (the *qa-2* gene region [15] [Fig. 2D and data not shown]). In general, the ladder of bands from ≈1.5 to 4 kb in the *Sau3AI* lanes of Fig. 2A indicate a heterogeneous population of molecules with methylation at some fraction of the numerous sites in the *am* region. Thus, the digests do not simply reflect a mixture of unmethylated and completely methylated molecules. Similar results were obtained with other enzymes sensitive to cytosine methylation, including *MspI* (Fig. 3C and D), *AvaI*, and *HhaI* (data not shown). Because isoschizomers that are insensitive to cytosine methylation are not available for these enzymes, we compared the digests with those prepared from DNA samples of cultures grown in the presence of 5AC, which prevents methylation (22, 47).

To focus on the native copy of *am* in strains containing two copies and to ascertain the extent of methylation outside the duplication, we probed blots with the unique sequences flanking the native *am* locus (Fig. 2B and C). For brevity, the *am* alleles at the native locus in strains N664, N665, N666, N669, N672, N675, N676, N617, N679, and N680 are referred to as *am*^{RIP1}, *am*^{RIP2}, *am*^{RIP3}, *am*^{RIP4}, *am*^{RIP5}, *am*^{RIP6}, *am*^{RIP7}, *am*^{RIP8}, *am*^{RIP9}, and *am*^{RIP10}, respectively, throughout (Table 1). The 3- to 3.5-kb bands seen in the *Sau3AI* lanes of Fig. 2B and C (strong in *am*^{RIP5} to *am*^{RIP10} and weak in *am*^{RIP3} and *am*^{RIP4}) result from blockage of all *Sau3AI* sites in the 2.6-kb *BamHI* fragment but cleavage within 1 kb on either side of this *BamHI* fragment (Fig. 2E). The prominent 800-bp bands in the *MboI* and *Sau3AI* lanes in Fig. 2B result from cutting at a site approximately 900 bp upstream of the duplication and one of two sites approximately 90 bp upstream of the duplication. No methylation was detected at these two sites in *am*^{RIP1} and

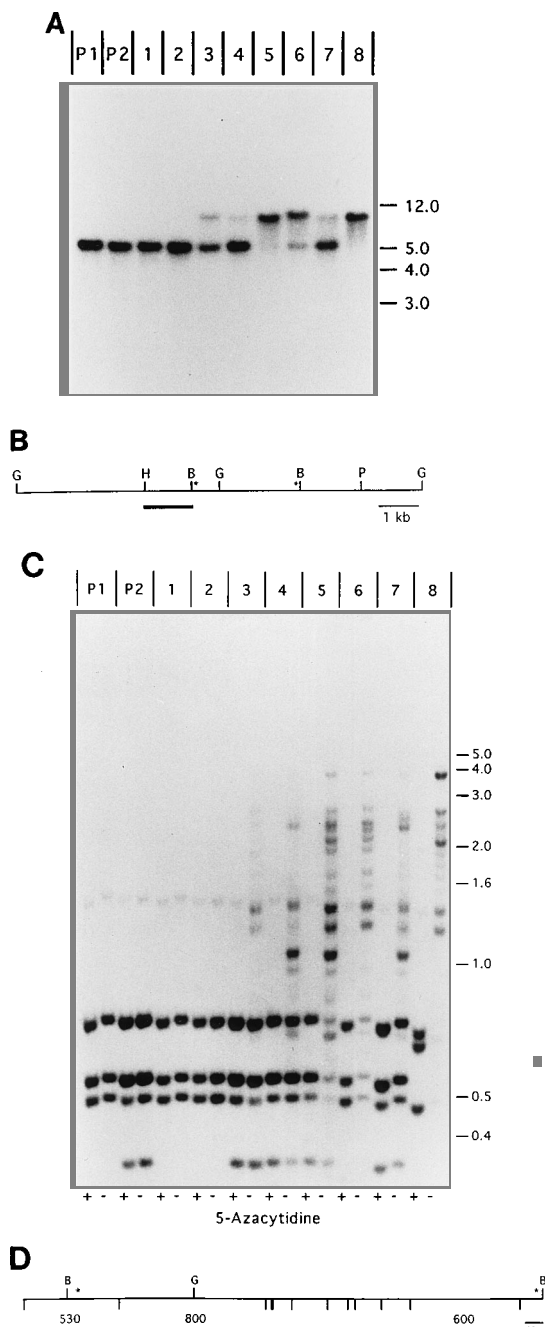


FIG. 3. Verification of methylation in *am^{RIP}* alleles at the native locus, and methylation at *MspI* sites. (A) Southern hybridization of genomic DNA samples from eight strains containing *am^{RIP}* alleles (lanes 1 to 8) or parent strains containing one or two copies of *am* (lanes P1 and P2), digested with *BglII* and probed with the *HindIII*-*BamHI* fragment corresponding to the unique sequences upstream of the native *am* gene. (B) Map indicating the *BamHI* (B), *BglII* (B), *HindIII* (H), and *PstI* (P) sites in wild-type *am*, the duplication boundaries (asterisk), and the probe (thick line). (C) Southern hybridization of DNA samples from cultures grown with (+) or without (-) 5AC, digested with *MspI*, and probed with the 2.6-kb *BamHI* fragment. (D) Map of *am* showing the *MspI* sites (below the horizontal line) and the sizes of the expected fragments (in base pairs) corresponding to the visible bands in wild-type *am*.

am^{RIP2}. Very little methylation was detected in *am^{RIP3}* and *am^{RIP4}*, and heavier, but incomplete methylation was found in *am^{RIP5}* to *am^{RIP10}*. Probing of the same blot with fragments from farther upstream and downstream of the duplication re-

vealed light methylation at *Sau3AI* sites 900 bp upstream and 570 bp downstream of the duplication in *am^{RIP3}* to *am^{RIP10}* (data not shown).

To confirm the methylation in *am^{RIP3}* and *am^{RIP4}* and to compare the degrees of methylation in the methylated *am^{RIP}* alleles, we used *BglII*, which has one site in the duplicated region, and probed with the unique DNA 5' to the duplicated segment of *am* (Fig. 3A). Cleavage of the *BglII* site in *am* results in an \approx 5-kb fragment, while blockage of this site results in an \approx 10-kb fragment. The *am^{RIP3}* to *am^{RIP8}* alleles were all methylated at the *BglII* site; however, the degree of methylation differed significantly. The detection of both 5- and 10-kb fragments in *am^{RIP3}* to *am^{RIP7}* reflects heterogeneity at the *BglII* site within the clonal cultures. In *am^{RIP5}*, *am^{RIP4}*, and *am^{RIP7}*, the majority of the hybridization was in the 5-kb band, indicating that a minority of the molecules was methylated at the *BglII* site. A greater fraction of the molecules was methylated at the *BglII* sites in *am^{RIP5}* and *am^{RIP6}*, and this site appeared to be completely methylated in *am^{RIP8}* (Fig. 3A).

Remethylation after 5AC treatment. The presence of methylation at *am* in the mutant strains could be explained in two ways. (i) Methylation arose in the sexual cycle and was then maintained by a system that depends upon existing methylation for its propagation in vegetative cells (maintenance methylation). (ii) RIP created a signal for de novo DNA methylation that works in vegetative cells; thus, the methylation reflected de novo methylation after every replication cycle (reiterative de novo methylation). To distinguish between these possibilities, we tested whether methylation would return after being prevented by growth in the presence of 5AC. DNA samples were prepared from 5AC cultures and from cultures grown after one passage in the absence of the drug. The 5AC treatment caused almost complete loss of methylation, as expected (Fig. 4). The alleles *am^{RIP5}* to *am^{RIP8}* regained methylation after 5AC treatment, suggesting that these alleles directed de novo methylation. In contrast, the *am* alleles at neither the native (*am^{RIP3}* and *am^{RIP4}*) nor the ectopic (*am^{RIPec3}* and *am^{RIPec4}*) loci in strains N666 and N669 regained methylation. Propagation of these two strains for three more passages without 5AC did not result in methylation (data not shown). These results suggest that the methylation at *am* in two of six mutant strains was propagated by a maintenance methylation system not limited to CpG dinucleotides.

De novo methylation of some *am^{RIP}* alleles occurs after reintroduction into vegetative *N. crassa* cells. It was conceivable that the remethylation observed in the previous experiment was dependent on residual methylation that remained after 5AC treatment. In addition, remethylation in *am^{RIP5}* and *am^{RIP7}* might have required the presence of ectopic copies of *am*. To address these possibilities, we asked whether completely unmethylated *am^{RIP}* alleles placed at the native *am* locus would induce de novo methylation in vegetative *N. crassa* cells lacking homologous sequences. We used a gene replacement system (26) to target *am^{RIP}* alleles to the native *am* locus. The transforming DNA was amplified in *E. coli* and was thus unmethylated except at *dcm*, *hsd*, and *dam* sites. Two or more independent *Am^r* transformants of *N. crassa* N408 were selected to represent each construct. To verify that each of the transformants contained a clean replacement at *am*, we compared the sizes of *am* fragments in digests of the transformants and the host strain using enzymes that cleave outside the region of interest. A 6-kb *PstI* fragment was detected in the *am* region of the host strain and in the transformants generated with *am^{RIP3}*, *am^{RIP4}*, *am^{RIP5}*, and *am^{RIP7}* DNA (Fig. 5A). Therefore, no *am* sequences integrated ectopically, and no net deletion or insertion occurred at the *am* loci in these transfor-

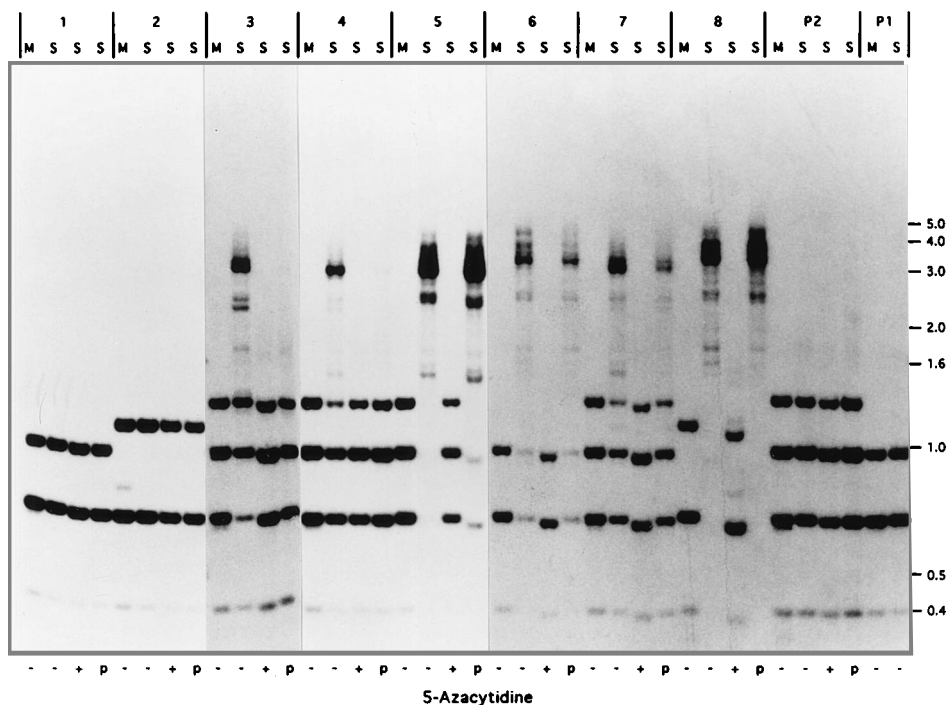


FIG. 4. Some *am^{RIP}* alleles undergo de novo methylation after 5AC treatment. Four genomic DNA samples of strains N664 (*am^{RIP1}* [set 1]), N665 (*am^{RIP2}* [set 2]), N666 (*am^{RIP3}* [set 3]), N669 (*am^{RIP4}* [set 4]), N672 (*am^{RIP5}* [set 5]), N675 (*am^{RIP6}* [set 6]), N676 (*am^{RIP7}* [set 7]), N617 (*am^{RIP8}* [set 8]), and N276 (parental duplicate *am* strain [set P2]) and two samples of N150 (wild type [set P1]) were digested with *Mbo*I (M) or *Sau*3AI (S), processed for Southern hybridization, and probed with the 2.6-kb *Bam*HI fragment of *am*. From left to right are two DNA samples prepared from normally grown tissue (-), from cultures grown in the presence of 5AC (+), and from cultures grown subsequently without 5AC treatment (p).

ments. *Pvu*II was used to test transformants that were generated with *am^{RIP8}* DNA, because RIP had created a *Pst*I site in *am^{RIP8}*.

To verify that the transforming DNA replaced the native *am* gene, we took advantage of restriction site changes created by RIP. *Mse*I was used to demonstrate that a mutation characteristic of *am^{RIP7}* is present in transformants N677 and N678 (Fig. 5B) and a mutation characteristic of *am^{RIP3}* is present in transformants N667 and N668. In addition, mutations at nucleotide positions 428 and 2031 in *am^{RIP3}* were verified in transformants N667 and N668 by using *Alu*I and *Eco*RI (data not shown). These mutations flank 41 of the 45 mutations in *am^{RIP3}* (sequence data described below). Allele *am^{RIP5}* contains two novel *Hind*III sites, and these sites were verified in N673 and N674 (Fig. 5B). A mutation at position 2356 in *am^{RIP8}* destroyed an *Mbo*I site and resulted in loss of the 1.0-kb fragment and gain of the 1.2-kb *Mbo*I fragment (Fig. 5C). Transformants N662 and N663 show this characteristic *Mbo*I fragment. The native site allele in *am^{RIP4}* has a novel 300-bp *Mbo*I fragment, and this fragment was detected in transformants N670 and N671. In addition, the 5'-most and 3'-most mutations in *am^{RIP4}* were verified in N670 by DNA sequencing as described in Materials and Methods.

Assays for methylation revealed that alleles *am^{RIP5}*, *am^{RIP7}*, and *am^{RIP8}* became methylated de novo in the respective transformants and that the methylation appeared to be equivalent to that in the strains from which the sequences were cloned (Fig. 5C). Thus, methylation of these alleles did not require prior methylation or the presence of an ectopic copy of *am*. Alleles *am^{RIP3}* and *am^{RIP4}* did not become methylated in the respective transformants, in keeping with the results of the 5AC experiment. We conclude that these alleles cannot trigger de novo methylation in vegetative cells.

DNA sequence analysis of *am^{RIP}* alleles. We determined the complete DNA sequences of *am^{RIP1}* to *am^{RIP8}* (Fig. 6). All mutations were G:C to A:T as expected from RIP (7). The numbers of mutations ranged from 8 to 158, resulting in 0.3 to 6.0% reduction of the G+C content in the duplicated segment of the *am* locus. Segments of *am^{RIP9}* and *am^{RIP10}* were also sequenced, and the density of mutations appeared to be at least as high as that in *am^{RIP8}* (data not shown). All of the mutations in *am^{RIP1}*, *am^{RIP3}*, *am^{RIP4}*, *am^{RIP6}*, and *am^{RIP7}* were G-to-A changes on the coding strand, and all of the mutations in *am^{RIP2}*, *am^{RIP5}*, and *am^{RIP8}* were C-to-T changes on the coding strand. Alleles *am^{RIP9}* and *am^{RIP10}* contain both G-to-A and C-to-T changes on the coding strand (data not shown). As expected on the basis of results of Southern hybridizations in previous studies (8), mutations identified in segments of ectopic alleles (*am^{RIPec3}*, *am^{RIPec4}*, *am^{RIPec5}*, and *am^{RIPec7}*) were not identical to those in their partners (data not shown). The mutations appeared to be randomly distributed, except for two aspects. The dinucleotide preference of RIP observed (CpA>>CpT>CpG>>CpC) was consistent with the results of previous studies (7). The density of mutations reflected the density of the preferred targets for RIP (CpA dinucleotides), except near the edges of the duplication, where the density of mutations was lower. The spacing between mutations appeared to be random, when codon usage was accounted for. Two mutations in *am^{RIP8}* occurred outside the duplication boundary (Fig. 7).

Of the eight *am^{RIP}* alleles that we sequenced completely, only *am^{RIP1}* lacks nonsense mutations. Most mutations were silent in alleles that had only C-to-T changes on the coding strand. Of 157 C-to-T changes on the coding strand, 117 (75%) were silent, 24 (15%) were missense, and 16 (10%) were nonsense mutations. In contrast, of 186 G-to-A changes on the

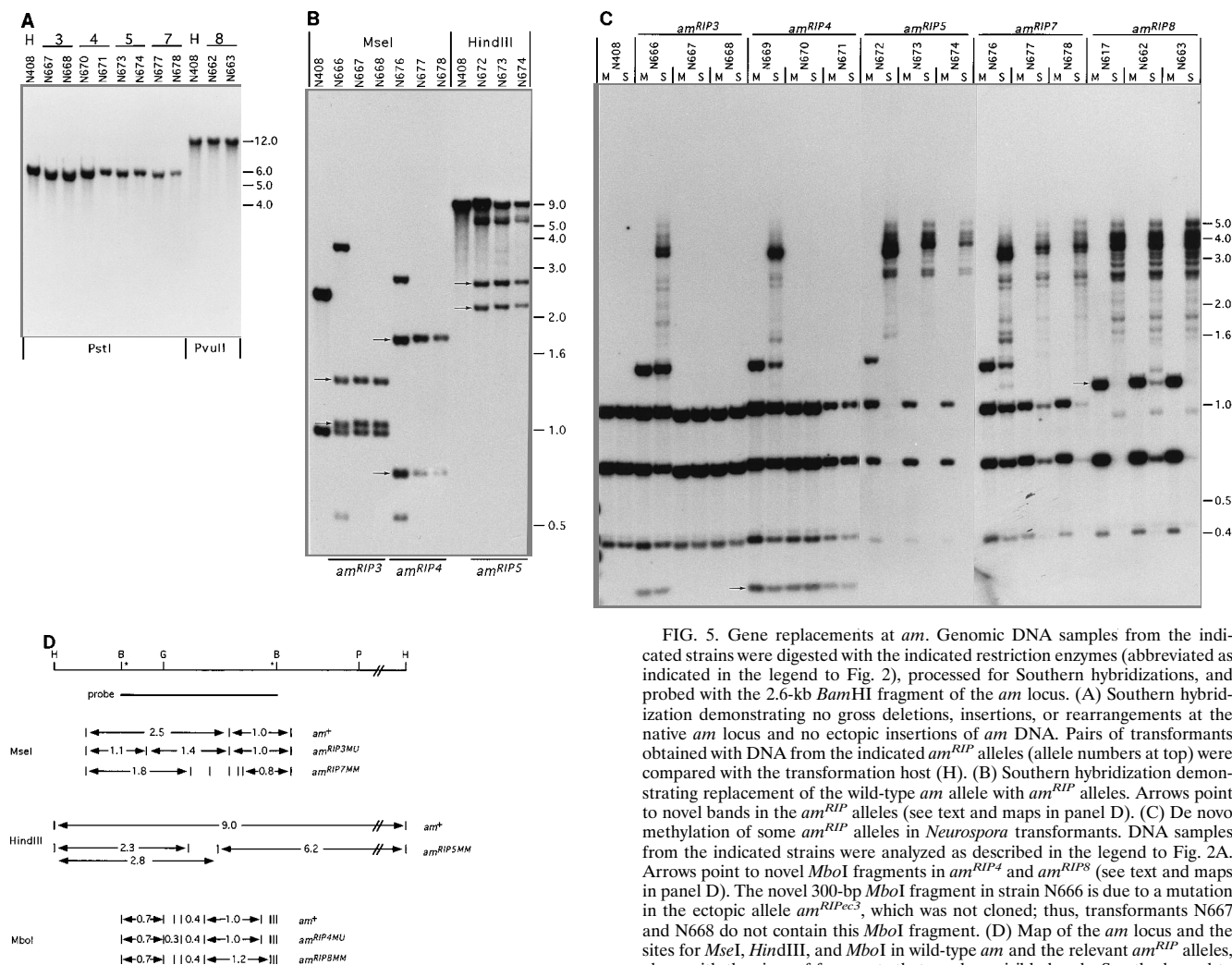


FIG. 5. Gene replacements at *am*. Genomic DNA samples from the indicated strains were digested with the indicated restriction enzymes (abbreviated as indicated in the legend to Fig. 2), processed for Southern hybridizations, and probed with the 2.6-kb *Bam*HI fragment of the *am* locus. (A) Southern hybridization demonstrating no gross deletions, insertions, or rearrangements at the native *am* locus and no ectopic insertions of *am* DNA. Pairs of transformants obtained with DNA from the indicated *amRIP* alleles (allele numbers at top) were compared with the transformation host (H). (B) Southern hybridization demonstrating replacement of the wild-type *am* allele with *amRIP* alleles. Arrows point to novel bands in the *amRIP* alleles (see text and maps in panel D). (C) De novo methylation of some *amRIP* alleles in *Neurospora* transformants. DNA samples from the indicated strains were analyzed as described in the legend to Fig. 2A. Arrows point to novel *Mbo*I fragments in *amRIP4* and *amRIP8* (see text and maps in panel D). The novel 300-bp *Mbo*I fragment in strain N666 is due to a mutation in the ectopic allele *amRIPec3*, which was not cloned; thus, transformants N667 and N668 do not contain this *Mbo*I fragment. (D) Map of the *am* locus and the sites for *Mse*I, *Hind*III, and *Mbo*I in wild-type *am* and the relevant *amRIP* alleles, along with the sizes of fragments that produce visible bands. See the legend to Fig. 7 for definitions of the letters *M* and *U* in the allele designations.

coding strand, 20 (11%) were silent, 151 (81%) were missense, and 16 (9%) were nonsense mutations. This difference is attributable to codon usage. Cytosine occupies the third position in 50% of the *am* codons, and guanosine occupies the first position in 40% of the *am* codons.

DNA sequence analyses. We carried out a variety of analyses to investigate why alleles *amRIP5* to *amRIP8* direct de novo methylation, unlike *amRIP1* to *amRIP4*, wild-type *am*, and apparently the bulk of the *Neurospora* genome. The correlation between methylation and the severity of RIP led us to consider A+T density and TpA density as potential determinants for methylation (Table 2). We determined the A+T contents of the *amRIP* sequences in windows of 10, 20, 40, 50, 100, 200, 400, 500, 700, or 1,000 bp. The various alleles showed similar base composition patterns, as illustrated with plots from analyses with 100-bp windows (Fig. 8). Maximum A+T density and TpA density values for each allele, at representative window sizes, are shown in Table 2. Alleles *amRIP5* to *amRIP8* have higher peak densities of A+T in 500-, 700-, and 1,000-bp segments than any known unmethylated *Neurospora* sequences (see Materials and Methods). At smaller window sizes, some unmethylated *Neurospora* sequences have higher densities of A+T than *amRIP5* to *amRIP8*. Similar analyses were performed

to examine TpA density in *amRIP* alleles. At window sizes of 600 and 1,000 bp, *amRIP5* to *amRIP8* contain higher densities of TpA than *amRIP1* to *amRIP4* and all other known unmethylated *Neurospora* sequences. No obvious correlation was observed between methylation and the frequency of any other dinucleotides or any trinucleotides.

The density of A+T varies greatly across the *am* gene in the wild-type allele. The differences between alleles appear relatively insignificant against the variation seen across the *am* gene. Intrinsic DNA bends are associated with periodically spaced A+T tracts (18). To explore the possibility that RIP created intrinsic DNA bends, we analyzed the *amRIP* sequences with the Gentben program (58). No bent regions were predicted in the wild-type *am* gene or any *amRIP* alleles.

We also compared the helical instability of the methylated and unmethylated *am* alleles using the Thermodyn program described by Miller and Kowalski (27). This program calculates the free-energy requirement for DNA strand separation on the basis of known thermodynamic properties of nearest-neighbor dinucleotides. No obvious distinction between the methylated and unmethylated alleles was detected with this program (data not shown).

Computer algorithms were used to search for oligonucleo-

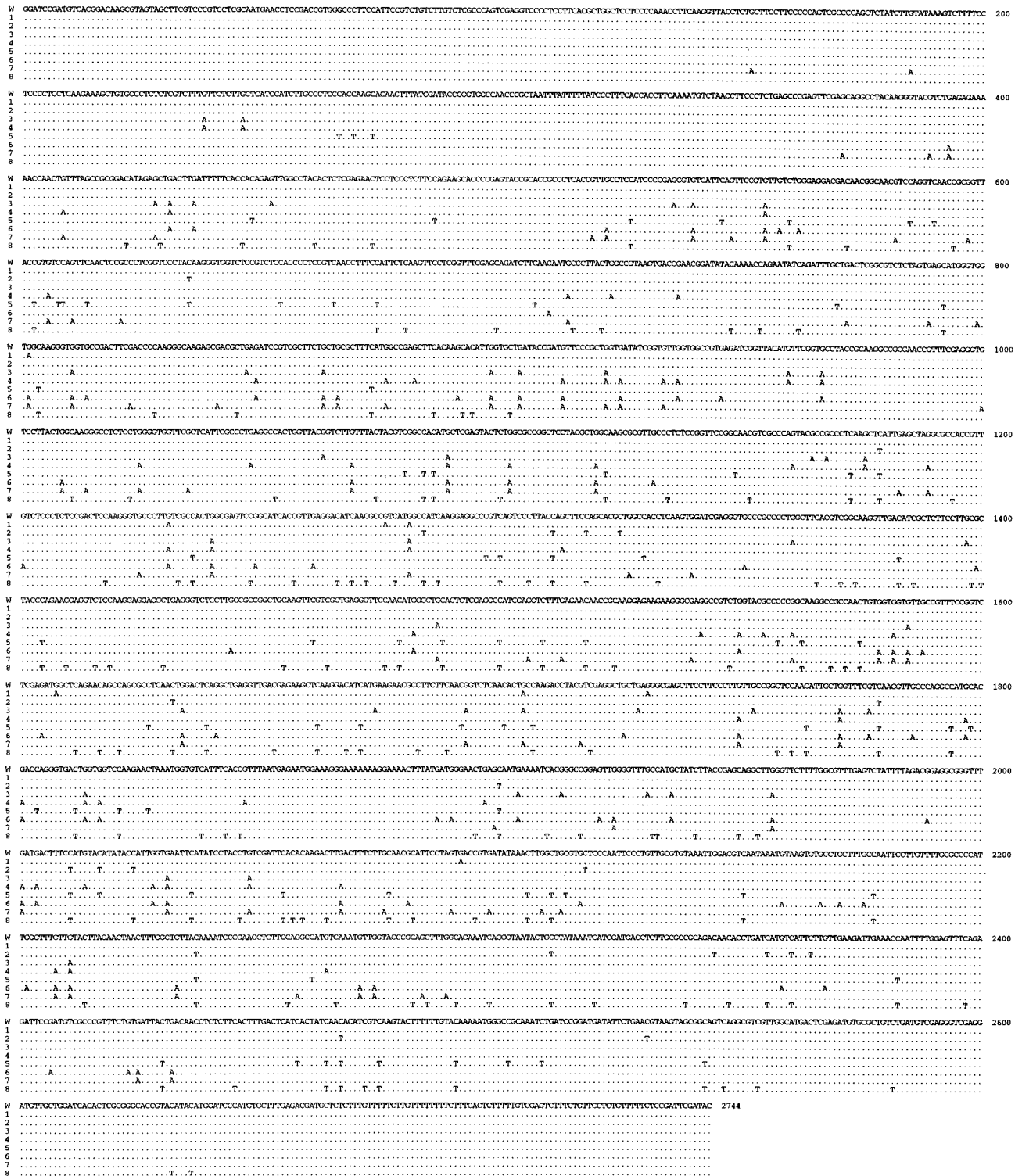


FIG. 6. DNA sequences of *am*^{RIP} alleles. The wild-type sequence (W) is shown in full (top), and identity with the mutant alleles (1 to 8) is indicated by dots. Mutations in the alleles are indicated by the appropriate letters. The numbering system is according to the published sequence of the 2.6-kb *Bam*HI fragment (23). Differences from the published sequence and GenBank mistakes are mentioned by Selker et al. (43). A 100-bp total of new sequence, outside the downstream *Bam*HI site, is shown. Alleles *am*^{RIP2}, *am*^{RIP3}, and *am*^{RIP6} and the functional allele of *am* from which they were derived (in N250) contain three additional nucleotides, CTC, in the 3' noncoding region of *am* (after nucleotide 2151).

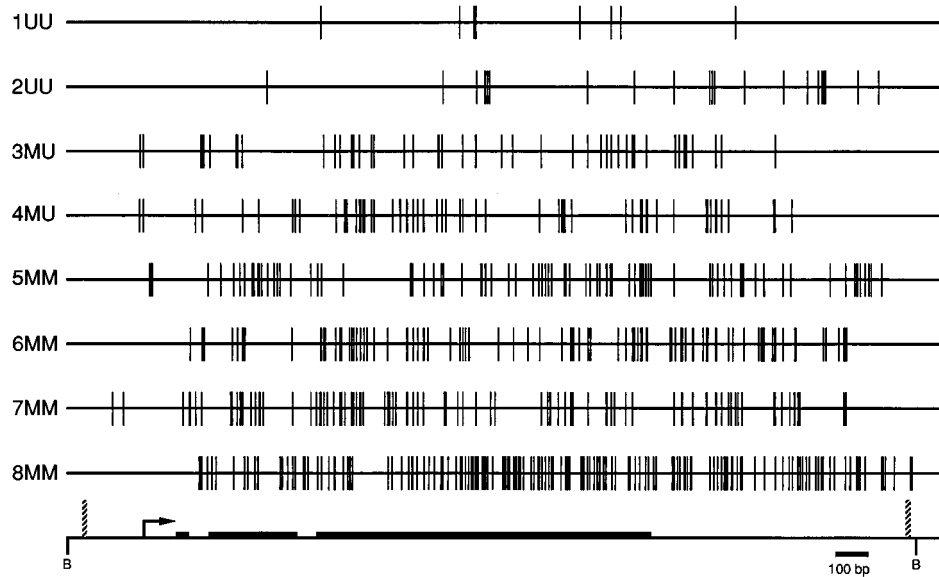


FIG. 7. Diagram of mutations in eight am^{RIP} alleles and a map representing features of the am gene. Vertical slashes represent mutations in the alleles. M (methylated) and U (unmethylated) refer, respectively, to the methylation status of the allele in the strain initially isolated and to the methylation status after 5AC treatment and subsequent growth in the absence of the drug. The horizontal line at the bottom represents the 2.7-kb region that was sequenced, including the 2.6-kb Bam HI fragment and 100 bp downstream. Exons (thick bars) of the am gene, the extent of the duplication (striped bars), transcription start site (arrow), and a scale bar are indicated.

tide sequences (5 to 20 bp) common to am^{RIP5} to am^{RIP8} but absent in wild-type am and am^{RIP1} to am^{RIP4} (see Materials and Methods). Several candidate oligonucleotide sequences were identified in the initial searches; however, these sequences also occur in *Neurospora* genes that are not methylated. We also performed the reverse analysis and found no oligonucleotide sequence in unmethylated sequences that is absent in all methylated sequences.

TABLE 2. Statistics for methylated and unmethylated sequences

| Allele ^a | No. of mutations ^b | Maximum A+T content (%) | | | Maximum no. of TpA | |
|---------------------|-------------------------------|------------------------------|---------------------|---------------------|---------------------|---------------------|
| | | Entire sequence ^c | 100 bp ^d | 500 bp ^e | 100 bp ^f | 600 bp ^g |
| am^+ | 0 | 46 | 63 | 58 | 8 | 31 |
| am^{RIP1UU} | 8 | 46 | 63 | 58 | 9 | 32 |
| am^{RIP2UU} | 21 | 47 | 65 | 60 | 11 | 38 |
| am^{RIP3MU} | 45 | 48 | 66 | 58 | 10 | 38 |
| am^{RIP4MU} | 56 | 48 | 67 | 60 | 14 | 43 |
| am^{RIP5MM} | 84 | 49 | 70 | 62 | 13 | 46 |
| am^{RIP6MM} | 86 | 49 | 68 | 62 | 15 | 56 |
| am^{RIP7MM} | 86 | 49 | 67 | 62 | 15 | 48 |
| am^{RIP8MM} | 158 | 52 | 72 | 72 | 16 | 59 |
| qa | NA | 49 | 83 | 60 | 12 | 33 |
| θ | NA | 53 | 64 | 56 | 12 | 44 |
| ζ - η | NA | 67 | 89 | 77 | 26 | 116 |

^a See the legend to Fig. 7 for definitions of the letters M and U in the allele designations.

^b Number of mutations (by RIP) in the am alleles. NA, not applicable.

^c The A+T contents were calculated for am (2.6-kb Bam HI fragment), the unmethylated qa gene cluster (positions 1 to 5000), the unmethylated θ region (957 bp), and the methylated ζ - η region (1.6 kb).

^d Peak values of A+T contents in 100-bp windows.

^e Peak values of A+T contents in 500-bp windows.

^f Peak numbers of TpA dinucleotides in 100-bp windows.

^g Peak numbers of TpA dinucleotides in 600-bp windows.

DISCUSSION

We have been investigating the specificity and control of DNA methylation in *N. crassa*. Cytosine methylation is typically found in sequences altered by RIP (45), and results of previous work demonstrated that several products of RIP serve as portable signals for de novo methylation (8, 17, 26, 41). To investigate how related sequences differentially govern methylation, we carried out a systematic study of sequences altered by RIP. Among eight null am^{RIP} alleles examined, 0.3 to 6.0% of the G:C base pairs were mutated in a single sexual cycle. This range of mutation may be unusually low, since we biased our sampling against alleles that appeared to be the most severely altered. We found that C-to-T changes on the coding strand typically occur in the third base of codons and result in silent mutations. This is attributable to codon usage in *N. crassa*; codons with C in the final position are highly overrepresented (10). Therefore, when RIP causes relatively low numbers of C-to-T changes on only the coding strand, the impact on the protein may be subtle. Indeed, a weak allele of am has been generated by RIP (13).

The single polarity of mutations (G to A or C to T) with respect to the coding strand in eight alleles indicates that RIP causes only one type of mutation, as suggested previously from limited data (7, 21). It is formally possible that RIP acted on only one strand in these alleles; however, it seems simpler to suppose that RIP acted on both strands but that the resulting mismatches were not repaired. The finding of both polarities of mutations in the more heavily mutated sequences (am^{RIP9} and am^{RIP10} ; *flank* described by Cambareri et al. [8]) can be explained by multiple rounds of RIP in a sexual cycle. This would be consistent with the fact that RIP occurs in dikaryotic tissue that undergoes multiple divisions before karyogamy (31, 41).

The observations that methylation occurs at nonsymmetrical sites in *N. crassa* and that methylation is heterogeneous indicated that the methylation could not be propagated by a maintenance methylase in the manner proposed by Riggs (36) and

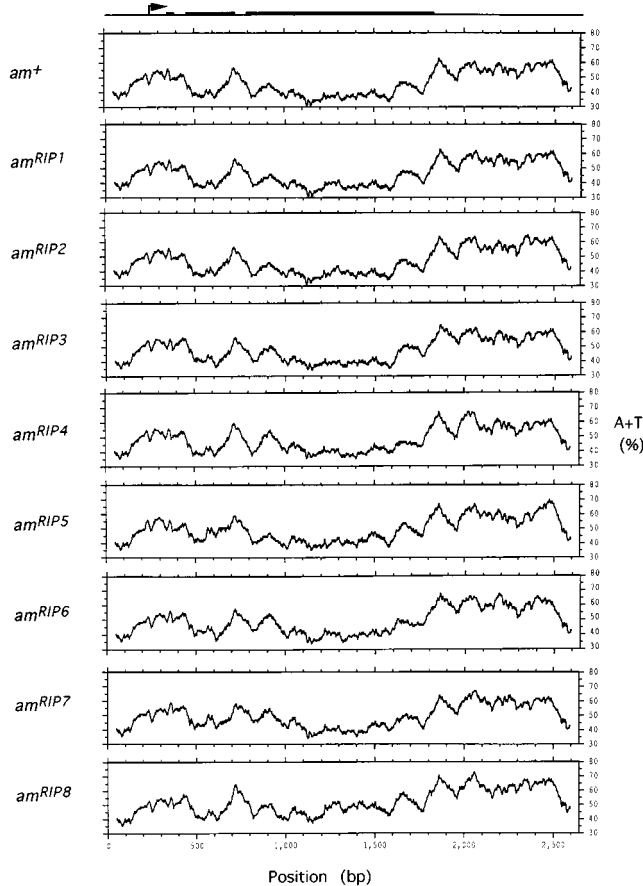


FIG. 8. Nucleotide compositions of am^+ and am^{RIP} alleles. The frequencies of A+T residues in successive 100-bp segments were calculated. The 100-bp window was moved along the $\approx 2,600$ bp sequences in 1-bp increments. The positions of exons (heavy lines) and the transcription start site (arrow) are indicated at the top.

Holliday and Pugh (20). These observations also raised the possibility that the methylation observed in *N. crassa* is due to reiterative de novo methylation. DNA-mediated transformation experiments, first with ζ - η (45, 46) and later with other products of RIP (8, 26), demonstrated sequence-dependent de novo methylation in vegetative *N. crassa* cells. Sequence-dependent de novo methylation in animal cells has also been observed (53, 55). We initiated this study to investigate the numbers and positions of mutations that are sufficient to induce de novo methylation. The am alleles in our collection with at least 84 mutations were substrates for de novo methylation, while am alleles with 56 or fewer mutations were not.

What is the trigger for de novo methylation in vegetative *Neurospora* cells at the DNA sequence level? Several models can be ruled out. No single mutation site is common to am^{RIP5} to am^{RIP8} ; therefore, no single nucleotide in am is a switch that regulates the methylation state of the locus. Mutations in the promoter region are apparently not necessary for methylation of am , since all mutations in am^{RIP6} and am^{RIP8} are at least 145 and 174 bp, respectively, downstream of the transcription start site. This finding suggests that the normal protein-DNA interactions in the promoter do not prevent methylation, in conflict with one class of models (39). The absence of transcription is not sufficient to trigger methylation, since unmethylated transcriptionally silent sequences have been identified (42, 47).

Models in which DNA methylation is triggered by a single, simple regulatory sequence do not easily account for the continuum of methylation levels observed. Nevertheless, we employed a number of approaches to explore the possibility that a single copy of an oligonucleotide sequence common to all methylated am alleles is the signal for de novo methylation in *N. crassa*. No candidate was found. The possibility remains that there are different signal sequences in different methylated regions. Models that involve multiple specific oligonucleotide sequences acting in concert to signal methylation are consistent with the data but difficult to test.

Models for de novo methylation involving highly degenerate discontinuous signals are most attractive because they can explain (i) the continuum of methylation levels observed and (ii) the high frequency with which rather nonspecific mutations, caused by RIP, create de novo methylation signals. Because RIP causes G:C-to-A:T changes and typically changes CpA to TpA, we considered the possibilities that methylation is signaled by (i) intrinsic DNA bends, (ii) high A+T density, (iii) helical instability, or (iv) high TpA density.

Periodically spaced tracts of A's and T's are associated with intrinsic DNA bends (for a review, see reference 18). No bends were predicted in any of the am^{RIP} alleles, suggesting that such structures are not involved in control of methylation in *Neurospora* cells. It is possible that some other type of DNA structure is crucial for establishment and/or maintenance of methylation. Z-DNA is stabilized by cytosine methylation (2), making it an attractive candidate for a self-stabilizing switch; however, it is not obvious that polarized transition mutations by RIP would generate sequences prone to adopting the Z form.

The G+C-rich CpG island sequences in mammalian DNA are relatively resistant to methylation by mouse DNA methyltransferase in vitro (3). It is possible that A+T-rich and/or TpA-rich DNA triggers de novo methylation, possibly by causing helical instability. The TpA dinucleotide is unusual in that it is underrepresented in all organisms that have been examined (6) and in that it has the lowest stacking energy of any dinucleotide (30). Could any DNA with a low melting point trigger DNA methylation? This might fit with the observation that the human cytosine methyltransferase recognizes unusual loose structures in vitro (51). Cytosine methylation raises the melting point of DNA (16), which should mitigate the effect RIP has on the melting properties of DNA.

Comparisons of the base compositions and the helical stabilities of methylated and unmethylated sequences did not reveal obvious candidates for methylation signals. Nevertheless, we found that segments of DNA 500 to 1,000 bp long from am^{RIP5} to am^{RIP8} , ζ - η , and $\psi 63$ have peak densities of A+T greater than any known unmethylated *Neurospora* sequences of the same sizes. Similarly, when measured in 600- to 1,000-bp segments, am^{RIP5} to am^{RIP8} , ζ - η , and $\psi 63$ have higher densities of TpA than am^{RIP1} to am^{RIP4} and all known unmethylated *N. crassa* sequences. However, it is not clear how the cell could differentiate between small differences in A+T and/or TpA density in gene-size tracts of DNA. A shortcoming of this model, in which a maximum density of A+T and/or TpA triggers methylation, is that it does not account for the observation that am^{RIP5} appears to be more heavily methylated than am^{RIP6} and am^{RIP7} . Perhaps a number of A+T-rich and/or TpA-rich segments influences methylation quantitatively and additively.

The simplest model for de novo methylation in *N. crassa* is that DNA sequences or structures created by RIP signal the methyltransferase directly. Alternatively, mutations resulting from RIP might cause methylation indirectly via alteration of

chromatin structure or by locally affecting a cellular process such as DNA replication. Late replication correlates with methylation in the inactive X chromosome and the fragile X site Xq27.3 (49); however, a causal relationship between methylation and replication timing is not clear.

On the basis of previous results with methylated *N. crassa* sequences (ζ - η [41], *flank* [7], and ψ 63 [26]), we expected that the primary sequence of all methylated *am* alleles would be able to direct de novo methylation. Therefore, we were surprised to discover that *am*^{RIP3} and *am*^{RIP4} (and the ectopic alleles from the same strains) were insufficient for de novo methylation in vegetative cells. The methylation in *am*^{RIP3} and *am*^{RIP4} presumably arose in the sexual cycle and was then somehow propagated. In the course of passaging the original *am*^{RIP3} strain (N666), we have noticed some instability of the methylation (unpublished data). Unstable methylation has also been observed in *N. crassa* at the *mtr* locus in unstable Mtr⁻ strains that arose spontaneously (51a, 52). Methylation in the *am*^{RIP4} to *am*^{RIP8} alleles was stable in vegetative passaging (data not shown). Our findings with *am*^{RIP3} and *am*^{RIP4} implicate a maintenance methylation system that is unlike the CpG-based system proposed to operate in animal cells (20, 36). The maintenance system may act on all methylated sequences in *Neurospora* cells; the efficiency of de novo methylation in sequences such as *am*^{RIP5} to *am*^{RIP8}, ζ - η , and ψ 63 makes it impossible to detect maintenance activity operating on these sequences.

The observation of methylation in *am*^{RIP3} and *am*^{RIP4} implicates de novo methylation in the *Neurospora* sexual cycle. It is not yet clear, however, whether cytosine methylation is part of the RIP mechanism. Two models for RIP are most appealing. (i) Some cytosines in duplicated sequences are deaminated to give uracils, and then replication fixes the mutations. (ii) Cytosines are methylated, and then some or all of these are deaminated to give thymines. On the basis of the suggestion that a suspected intermediate in the enzymatic methylation reaction is more than 10⁴ times more prone to spontaneous deamination than is cytosine (11, 61), we proposed that RIP may be catalyzed by a DNA methyltransferase under special conditions, such as when the methyl group donor *S*-adenosylmethionine is limiting (40). Supporting this model, recent studies have demonstrated that two bacterial cytosine methyltransferases can catalyze deamination (48, 62).

If one assumes that methylation occurred in all *am*^{RIP} alleles during the sexual cycle, the discovery of maintenance methylation in alleles with intermediate numbers of mutations, but not in alleles with the fewest mutations (*am*^{RIP1} and *am*^{RIP2}), raises the possibility that the maintenance system is not sequence independent. This was also suggested by failure to detect propagation of methylation in arbitrary wild-type sequences that were methylated in vitro and introduced into *N. crassa* by DNA-mediated transformation (7a). Our observation that the methylation of *am*^{RIP4} was more stable than that of *am*^{RIP3} further supports the suggestion of sequence-dependent maintenance methylation in *N. crassa*. One model for the establishment of methylation patterns in mammals is that all CpGs are methylated de novo at an early stage in development, but that the methylation of some CpGs is lost, depending on their sequence context (34). Indeed, imperfect maintenance of methylation at CpGs within in vitro-methylated transgenes was observed in numerous studies (19, 33, 59). The sequence context of CpGs may affect methylation maintenance indirectly through protein binding, DNA structure, or chromatin structure.

Observations made regarding *Ascobolus immersus* implied that this fungus also propagates methylation at nonsymmetri-

cal sites. The evidence came from the discovery of a process closely related to RIP, which is called methylation induced premeiotically (MIP [12, 35]). Like RIP, MIP inactivates duplicated sequences in a pairwise manner during the sexual stage of the life cycle. Unlike RIP, however, MIP does not cause mutations. Rather, sequences are inactivated by methylation. As in *Neurospora* cells, this methylation is not limited to symmetrical sites, and persistence of methylation does not require that the DNA remain duplicated. All sequences tested to date are subject to MIP, suggesting that in *Ascobolus* methylation is propagated by a maintenance system that is sequence independent. Thus, *Neurospora* and *Ascobolus* cells may have related mechanisms for methylation maintenance, but they differ in that the *Neurospora* system appears sequence dependent. It will be interesting to learn whether sequence-dependent maintenance methylation occurs in other organisms, such as mammals.

ACKNOWLEDGMENTS

This work was supported by NIH grant GM 35690 and NSF grant DCB 8718163 and was done during the tenure of an Established Investigatorship of the American Heart Association (E.U.S.).

We are grateful to John Anderson, Dave Hagen, and David Kowalski for computer software; and Phil Garrett-Engle, Brian Margolin, and Vivian Miao for technical assistance. We thank Adrian Bird, Jette Foss, Jeff Irelan, Jack Kinsey, and Vivian Miao for comments on the manuscript and members of the Selker laboratory and Rik Myers for fruitful discussions.

REFERENCES

1. Antequera, F., and A. Bird. 1993. CpG Islands, p. 169–185. In J. P. Jost and H. P. Saluz (ed.), DNA methylation: molecular biology and biological significance, vol. 64. Birkhäuser Verlag, Boston.
2. Behe, M., S. Zimmerman, and G. Felsenfeld. 1981. Changes in the helical repeat of poly(dG-m⁵dC) · poly(dG-m⁵dC) and poly(dG-dC) · poly(dG-dC) associated with the B-Z transition. *Nature (London)* **293**:233–235.
3. Bestor, T. H., G. Gundersen, A.-B. Kolstø, and H. Pyrdz. 1992. CpG islands in mammalian gene promoters are inherently resistant to de novo methylation. *Genet. Anal. Tech. Appl.* **9**:48–53.
4. Bird, A. P. 1993. Imprints on islands. *Curr. Biol.* **3**:275–277.
5. Brandeis, M., D. Frank, I. Keshet, Z. Siegfried, M. Mendelsohn, A. Nemes, V. Temper, A. Razin, and H. Cedar. 1994. Sp1 elements protect a CpG island from de novo methylation. *Nature (London)* **371**:435–438.
6. Burge, C., A. M. Campbell, and S. Karlin. 1992. Over- and underrepresentation of short oligonucleotides in DNA sequences. *Proc. Natl. Acad. Sci. USA* **89**:1358–1362.
7. Cambareri, E. B., B. C. Jensen, E. Schabtach, and E. U. Selker. 1989. Repeat-induced G-C to A-T mutations in *Neurospora*. *Science* **244**:1571–1575.
- 7a. Cambareri, E. B., S. Lommel, B. Margolin, V. Miao, and E. Selker. Unpublished data.
8. Cambareri, E. B., M. J. Singer, and E. U. Selker. 1991. Recurrence of repeat-induced point mutation (RIP) in *Neurospora crassa*. *Genetics* **127**:699–710.
9. Davis, R. H., and F. J. De Serres. 1970. Genetic and microbiological research techniques for *Neurospora crassa*. *Methods Enzymol.* **17**:47–143.
10. Edelmann, S. E., and C. Staben. 1994. A statistical analysis of sequence features within genes from *Neurospora crassa*. *Exp. Mycol.* **18**:70–81.
11. Evans, B. E., G. N. Mitchell, and R. Wolfenden. 1975. The action of bacterial cytidine deaminase on 5,6-dihydrocytidine. *Biochemistry* **14**:621–624.
12. Faugeron, G., L. Rhounim, and J.-L. Rossignol. 1990. How does the cell count the number of ectopic copies of a gene in the premeiotic inactivation process acting in *Ascobolus immersus*? *Genetics* **124**:585–591.
13. Fincham, J. R. 1990. Generation of new functional mutant alleles by premeiotic disruption of the *Neurospora crassa* *am* gene. *Curr. Genet.* **18**:441–445.
14. Foss, H. M., C. J. Roberts, K. M. Claeys, and E. U. Selker. 1993. Abnormal chromosome behavior in *Neurospora* mutants defective in DNA methylation. *Science* **262**:1737–1741.
- 14a. Garrett-Engle, P., M. Singer, and E. Selker. Unpublished data.
15. Giles, N. H., M. E. Case, J. Baum, R. Geever, L. Huiet, V. Patel, and B. Tyler. 1985. Gene organization and regulation in the *qa* (quinic acid) gene cluster of *Neurospora crassa*. *Microbiol. Rev.* **49**:338–358.

16. Gill, J. E., J. A. Mazrimas, and C. C. Bishop, Jr. 1974. Physical studies on synthetic DNAs containing 5-methylcytosine. *Biochim. Biophys. Acta* **335**: 330–348.
17. Grayburn, W. S., and E. U. Selker. 1989. A natural case of RIP: degeneration of DNA sequence in an ancestral tandem duplication. *Mol. Cell. Biol.* **9**: 4416–4421.
18. Hagerman, P. J. 1990. Sequence-directed curvature of DNA (II). *Annu. Rev. Biochem.* **59**:755–781.
19. Harland, R. 1982. Inheritance of DNA methylation in microinjected eggs of *Xenopus laevis*. *Proc. Natl. Acad. Sci. USA* **79**:2323–2327.
20. Holliday, R., and J. E. Pugh. 1975. DNA modification mechanisms and gene activity during development. *Science* **187**:226–232.
21. Jarai, G., and G. A. Marzluf. 1991. Generation of new mutants of *nmr*, the negative-acting nitrogen regulatory gene of *Neurospora crassa*, by repeat induced mutation. *Curr. Genet.* **20**:284–288.
22. Jones, P. A. 1984. Gene activation by 5-azacytidine, p. 165–187. *In* A. Razin, H. Cedar, and A. D. Riggs (ed.), *DNA methylation: biochemistry and biological significance*. Springer-Verlag, New York.
23. Kinnaird, J. H., and J. R. S. Fincham. 1983. The complete nucleotide sequence of the *Neurospora crassa am* (NADP-specific glutamate dehydrogenase) gene. *Gene* **26**:253–260.
24. Li, E., T. H. Bestor, and R. Jaenisch. 1992. Targeted mutation of the DNA methyltransferase gene results in embryonic lethality. *Cell* **69**:915–926.
25. Macleod, D., J. Charlton, J. Mullins, and A. P. Bird. 1994. Sp1 sites in the mouse *aprt* gene promoter are required to prevent methylation of the CpG island. *Genes Dev.* **8**:2282–2292.
- 25a. Marcotte, B. Unpublished data.
- 25b. Margolin, B., D. Fritz, J. Stevens, P. Garrett-Engele, C. Garrett-Engele, R. Metzberg, and E. Selker. Unpublished data.
26. Miao, V. P. W., M. J. Singer, M. R. Rountree, and E. U. Selker. 1994. A targeted replacement system for identification of signals for de novo methylation in *Neurospora crassa*. *Mol. Cell. Biol.* **14**:7059–7067.
27. Miller, C. A., and D. Kowalski. 1993. *cis*-acting components in the replication origin from ribosomal DNA of *Saccharomyces cerevisiae*. *Mol. Cell. Biol.* **13**:5360–5369.
28. Monk, M., M. Boubelik, and S. Lehnert. 1987. Temporal and regional changes in DNA methylation in the embryonic, extraembryonic and germ cell lineages during mouse embryo development. *Development* **99**:371–382.
29. Nelson, M., E. Raschke, and M. McClelland. 1993. Effect of site-specific methylation on restriction endonucleases and DNA modification methyltransferases. *Nucleic Acids Res.* **21**:3139–3154.
30. Ornstein, R. L., R. Rein, D. L. Breen, and R. D. Macelroy. 1978. An optimized potential function for the calculation of nucleic acid interaction energies. I. Base stacking. *Biopolymers* **17**:2341–2360.
31. Perkins, D. D., and E. D. Barry. 1977. The cytogenetics of *Neurospora*. *Adv. Genet.* **19**:133–285.
32. Perkins, D. D., R. L. Metzberg, N. B. Raju, E. U. Selker, and E. G. Barry. 1986. Reversal of a *Neurospora* translocation by crossing over involving displaced rDNA, and methylation of the rDNA segments that result from recombination. *Genetics* **114**:791–817.
33. Pollack, Y., R. Stein, A. Razin, and H. Cedar. 1980. Methylation of foreign DNA sequences in eukaryotic cells. *Proc. Natl. Acad. Sci. USA* **77**:6463–6467.
34. Razin, A., and A. Riggs. 1980. DNA methylation and gene function. *Science* **210**:604–610.
35. Rhounim, L., J.-L. Rossignol, and G. Faugeron. 1992. Epimutation of repeated genes in *Ascobolus immersus*. *EMBO J.* **11**:4451–4457.
36. Riggs, A. D. 1975. X-inactivation, differentiation and DNA methylation. *Cytogenet. Cell Genet.* **14**:9–25.
37. Russell, P. J., K. D. Rodland, J. E. Cutler, E. M. Rachlin, and J. A. McClosley. 1985. DNA methylation in *Neurospora*: chromatographic and isochizomer evidence for changes during development, p. 321–332. *In* W. Timberlake (ed.), *Molecular genetics of filamentous fungi*. Alan R. Liss, Inc., New York.
38. Sasaki, H., N. D. Allen, and M. A. Surani. 1993. DNA methylation and genomic imprinting in mammals, p. 469–486. *In* J. P. Jost, and H. P. Saluz (ed.), *DNA methylation: molecular biology and biological significance*, vol. 64. Birkhäuser Verlag, Boston.
39. Selker, E. 1990. DNA methylation and chromatin structure: a view from below. *Trends Biochem. Sci.* **15**:103–107.
- 39a. Selker, E., N. Tauntas, B. Margolin, S. Cross, and A. Bird. Unpublished data.
40. Selker, E. U. 1990. Premeiotic instability of repeated sequences in *Neurospora crassa*. *Annu. Rev. Genet.* **24**:579–613.
41. Selker, E. U., E. B. Cambareri, B. C. Jensen, and K. R. Haack. 1987. Rearrangement of duplicated DNA in specialized cells of *Neurospora*. *Cell* **51**:741–752.
42. Selker, E. U., S. J. Free, R. L. Metzberg, and C. Yanofsky. 1981. An isolated pseudogene related to the 5S RNA genes in *Neurospora crassa*. *Nature (London)* **294**:576–577.
43. Selker, E. U., D. Y. Fritz, and M. J. Singer. 1993. Dense non-symmetrical DNA methylation resulting from repeat-induced point mutation (RIP) in *Neurospora*. *Science* **262**:1724–1728.
44. Selker, E. U., and P. W. Garrett. 1988. DNA sequence duplications trigger gene inactivation in *Neurospora crassa*. *Proc. Natl. Acad. Sci. USA* **85**:6870–6874.
45. Selker, E. U., B. C. Jensen, and G. A. Richardson. 1987. A portable signal causing faithful DNA methylation *de novo* in *Neurospora crassa*. *Science* **238**:48–53.
46. Selker, E. U., G. A. Richardson, P. W. Garrett-Engele, M. J. Singer, and V. Miao. 1993. Dissection of the signal for DNA methylation in the ζ - η region of *Neurospora*. *Cold Spring Harbor Symp. Quant. Biol.* **58**:323–329.
47. Selker, E. U., and J. N. Stevens. 1985. DNA methylation at asymmetric sites is associated with numerous transition mutations. *Proc. Natl. Acad. Sci. USA* **82**:8114–8118.
48. Shen, J.-C., W. M. Rideout III, and P. A. Jones. 1992. High frequency mutagenesis by a DNA methyltransferase. *Cell* **71**:1073–1080.
- 48a. Singer, M., V. Miao, and E. Selker. Unpublished data.
49. Singer-Sam, J., and A. D. Riggs. 1993. X chromosome inactivation and DNA methylation, p. 358–384. *In* J. P. Jost and H. P. Saluz (ed.), *DNA methylation: molecular biology and biological significance*. Birkhäuser Verlag, Boston.
50. Sinsheimer, R. L. 1955. The action of pancreatic deoxyribonuclease. II. Isomeric dinucleotides. *J. Biol. Chem.* **215**:579–583.
51. Smith, S. S., J. L. C. Kan, D. J. Baker, B. E. Kaplan, and P. Dembek. 1991. Recognition of unusual DNA structures by human DNA (cytosine-5) methyltransferase. *J. Mol. Biol.* **217**:39–51.
- 51a. Stadler, D. Personal communication.
52. Stadler, D., H. Macleod, and D. Dillon. 1991. Spontaneous mutation at the *mtr* locus of *Neurospora*: the spectrum of mutant types. *Genetics* **129**: 39–45.
53. Szyf, M., B. P. Schimmer, and J. G. Seidman. 1989. Nucleotide-sequence-specific *de novo* methylation in a somatic murine cell line. *Proc. Natl. Acad. Sci. USA* **86**:6853–6857.
54. Toth, M., U. Müller, and W. Doerfler. 1990. Establishment of *de novo* DNA methylation patterns: transcription factor binding and deoxycytidine methylation at CpG and non-CpG sequences in an integrated adenovirus promoter. *J. Mol. Biol.* **214**:673–683.
55. Turker, M. S., P. Mummaneni, and P. L. Bishop. 1991. Region- and cell type-specific *de novo* DNA methylation in cultured mammalian cells. *Somat. Cell. Mol. Genet.* **17**:151–157.
56. Turker, M. S., K. Swisshelm, A. C. Smith, and G. M. Martin. 1989. A partial methylation profile for a CpG site is stably maintained in mammalian tissues and cultured cell lines. *J. Biol. Chem.* **264**:11632–11636.
57. Ulanovsky, L. E., and E. N. Trifonov. 1987. Estimation of wedge components in curved DNA. *Nature (London)* **326**:720–722.
58. VanWye, J. D., E. C. Bronson, and J. N. Anderson. 1991. Species-specific patterns of DNA bending and sequence. *Nucleic Acids Res.* **19**:5253–5261.
59. Wigler, M., D. Levy, and M. Perucho. 1981. The somatic replication of DNA methylation. *Cell* **24**:33–40.
60. Woodcock, D. M., P. J. Crowther, and W. P. Diver. 1987. The majority of methylated deoxycytidines in human DNA are not in the CpG dinucleotide. *Biochem. Biophys. Res. Commun.* **145**:888–894.
61. Wu, J. C., and D. V. Santi. 1987. Kinetic and catalytic mechanism of *HhaI* methyltransferase. *J. Biol. Chem.* **262**:4778–4786.
62. Wyszynski, M., S. Gabbara, and A. S. Bhagwat. 1994. Cytosine deaminations catalyzed by DNA cytosine methyltransferases are unlikely to be the major cause of mutational hot spots at sites of cytosine methylation in *Escherichia coli*. *Proc. Natl. Acad. Sci. USA* **91**:1574–1578.
63. Yisraeli, J., and M. Szyf. 1984. Gene methylation patterns and expression, p. 353–378. *In* A. Razin, H. Cedar, and A. D. Riggs (ed.), *DNA methylation: biochemistry and biological significance*. Springer, New York.